

# The effect of catalyst preparation conditions on the synthesis of menthol from citronellal on Ru/H-BEA



Jutta Plößer, Fatma Dedeaga, Martin Lucas, Peter Claus\*

Technical University Darmstadt, Dept. of Chemistry, Chemical Technology II, Alarich-Weiss-Straße 8, 64287 Darmstadt, Germany

## ARTICLE INFO

### Article history:

Received 11 December 2015  
Received in revised form 28 January 2016  
Accepted 11 February 2016  
Available online 12 February 2016

## ABSTRACT

Heterogeneous Ru/H-BEA catalysts are suitable catalysts for the one-pot transformation of citronellal to menthols, which requires a combined cyclization-hydrogenation step. Here, we report the role of different preparation conditions—namely the choice of the Ru-precursor ( $\text{Ru}(\text{NO})(\text{NO}_3)_3$ ),  $\text{Ru}(\text{acac})_3$ ,  $\text{RuCl}_3$  and  $\text{Ru}_3(\text{CO})_{12}$ ) as well as the reduction temperature (523–923 K) of the catalyst. Using  $\text{Ru}(\text{NO})(\text{NO}_3)_3$  as precursor the highest activity was obtained, while the product distribution was not strongly affected by the choice of the precursor.

On the contrary the reduction temperature leads to very different product distributions: Increasing it from 623 K to 923 K for a 1%Ru/H-BEA-25 catalyst the competitive hydrogenation of citronellal was diminished, which leads to an increased selectivity to menthols from 77% to 87% and additional the activity increases with a factor of 3.4. This behaviour might be due to a dealumination of the zeolite during reduction at higher temperatures. Moreover, in combination with appropriate reaction conditions a yield to menthols of 92% can be reached.

© 2016 Elsevier B.V. All rights reserved.

## 1. Introduction

Menthol is one of the world's most common aroma compounds, which is applied in pharmaceuticals, toothpastes, tobacco, chewing gums, cosmetics and confectionary [1,2]. Because of its three chiral centres in the cyclohexane ring, menthol has four stereoisomeric pairs. However only (−)-menthol has the typical strong odour and cooling effect. Therefore the other stereoisomers as well as (+)-menthol are less valuable [1].

A large part of the produced menthol is obtained by extraction from *Mentha arvensis* or *Mentha piperita* in India, China, Japan, Brazil and Taiwan [1,2].

In order to obtain synthetic menthol, it is necessary to either treat racemic menthol in a separation crystallization process (Haarmann-Reimer process) or use a chiral homogeneous catalyst (Takasago and BASF process) [1,2]. But usage of the latter is accompanied by disadvantages of homogeneous catalysis like catalyst separation and high prices for these catalysts. Therefore, the use of heterogeneous catalysts is an attractive alternative.

A promising route via heterogeneous catalysis starts from citronellal and involves two consecutive steps: the cyclization of

citronellal to isopulegols and a following hydrogenation to menthols (Fig. 1). During the first step—the cyclization of citronellal (Fig. 1, route 1)—the configuration on the three prochiral carbon atoms is formed. Therefore the catalyst should produce a huge excess of the desired stereoisomer. The double bond of isopulegols can be easily hydrogenated by conventional metal catalysts to produce menthols (Fig. 1, route 2).

Competitively to the cyclization, citronellal can be hydrogenated to citronellol, dihydrocitronellal and dimethyloctanol (summed up as hydrogenation products), which form the first group of undesired by-products to be prevented (Fig. 1, route 3). In addition isopulegols and menthols can be defunctionalized to obtain *p*-menthenes and *p*-menthanes. Furthermore citronellal and isopulegol can form dimers.

In prior studies the isolated cyclization of citronellal was investigated on supported or non-supported Lewis acids like  $\text{ZnBr}_2$ ,  $\text{ZnCl}_2$ ,  $\text{FeSO}_4$  [3–7], supported or non-supported heteropoly acids [8,9], sulfated or phosphated zirconia [10,11],  $\text{ZrO}_2$  dispersed in  $\text{SiO}_2$ –montmorillonite [12] and zeolites [10,13–16].  $\text{ZnBr}_2$  is highly active and produces the desired isopulegol with a diastereoselectivity of >90% [2,6,7]. But  $\text{ZnBr}_2$  is soluble under the given conditions and therefore the disadvantages of homogeneous catalysis prevail. In contrast H-BEA zeolites are promising solid acids for the cyclization of citronellal to isopulegol due to the high diastereoselectivity of about 70% and the small amounts of by-products [10,14,15,17].

\* Corresponding author.

E-mail address: [claus@tc2.tu-darmstadt.de](mailto:claus@tc2.tu-darmstadt.de) (P. Claus).

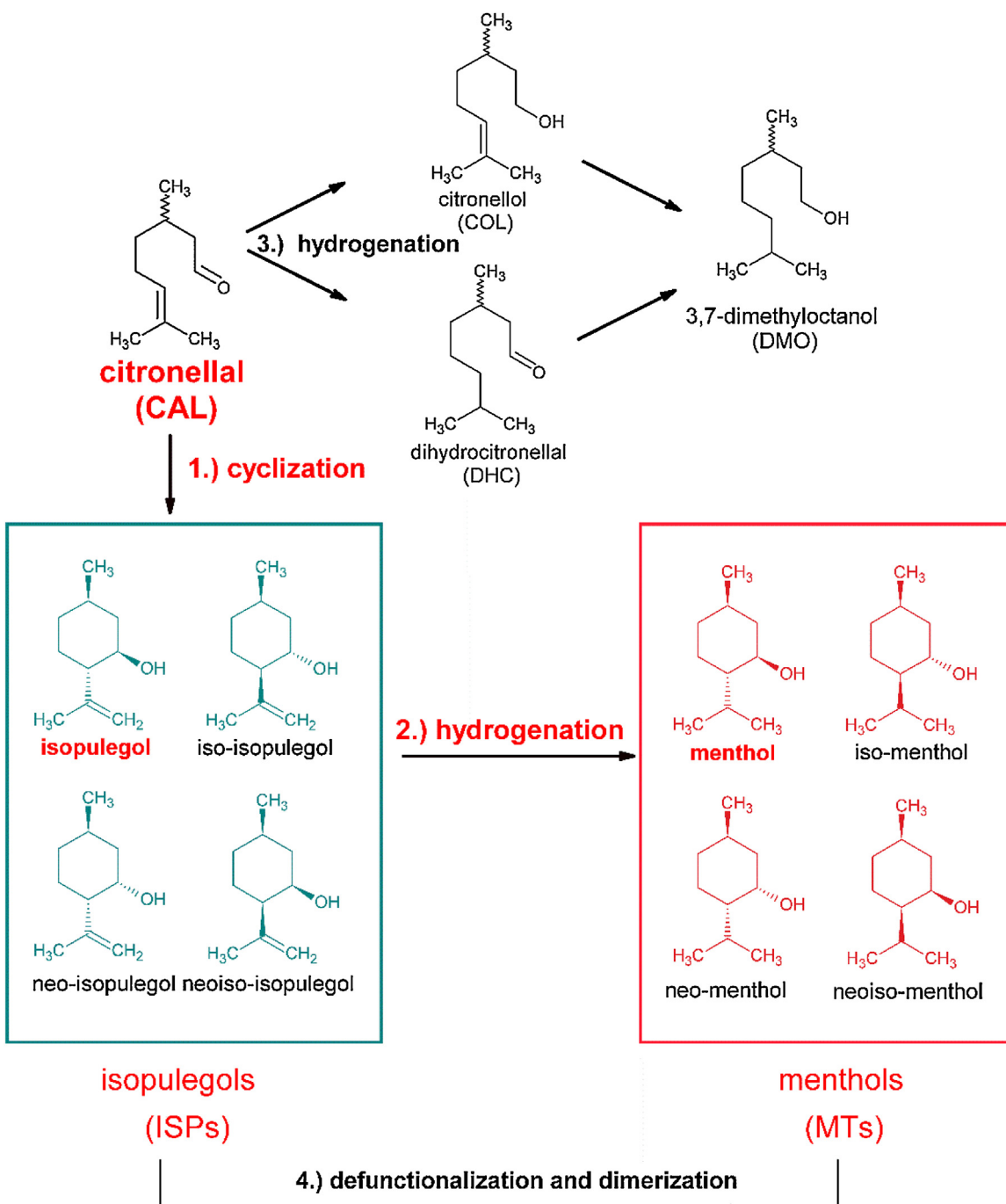


**Fig. 1.** Reaction network of the transformation of citronellal to menthol. Note that the name menthols involves the group of the menthol stereoisomers, whereas menthol is used for the enantiomeric menthol pair. Only one enantiomer is shown in each case.

To obtain menthols in a one-pot transformation from citronellal several bifunctional metal/solid acid catalysts and supported bifunctional systems have been investigated. Using physical mixtures of  $ZnBr_2/Al_2O_3$  &  $Ni/Al_2O_3$  menthol yields of 75% were obtained [18], whereas on bifunctional catalysts ( $Ru/ZnBr_2/SiO_2$  [19],  $Pt/Ga/MCM-41$  [20],  $Pd/H_3PW_{12}O_{40}/SiO_2$  [21]),  $Au/MgF_2$  [22] and metal/zeolite catalysts ( $Ni/Zr-BEA$  [23],  $Pt/H-BEA$  [24],  $Ir/H-BEA$  [7,25] and  $Ru/H-BEA$  [6]) selectivities of around 90% were reached. Using metal/H-BEA catalysts reaction conditions such as loading of the active metal, Si:Al ratio of the zeolite, temperature, hydrogen pressure and solvent had significant effects on the product distribution. Metal loading, hydrogen pressure and temperature showed the same dependencies for Ir [7], Pt [24] and Ru [6] cat-

alysts (at low loadings, low hydrogen pressures, and temperatures between 353 K and 373 K the highest selectivities to menthols were obtained) whereas the solvent proves to have different dependencies. Non-polar solvents like cyclohexane improve the menthols yield on Ir/H-BEA catalyst [7], whereas on Pt/H-BEA [24] and Ru/H-BEA [6] dioxane leads to the highest yields to menthols of 93%.

However the effect of the metal precursor and catalyst reduction temperature were not studied in detail. As shown for other catalyst systems these preparation procedures had a significant effect on the catalyst performances. The choice of the precursor can affect size and nature of metal particles as well as acidity of the support (for example due to residual  $Cl^-$  ions) [26,27]. A high temperature treatment of medium and large pore zeolites (especially zeolite BEA

[28]) lead to different levels of structural dealumination with formation of variable amounts of extraframework aluminium species (EF-Al) [29,30]. It was shown that catalytic performance of BEA zeolites can be influenced by the level of dealumination [28,31].

The present work systematically investigates the influence of the Ru precursor and the reduction temperature in the one-pot transformation of citronellal into menthols on Ru/H-BEA catalysts. Characterization was carried out by means of CO chemisorption, DRIFTS and Pyridine DRIFTS spectroscopy, XRD, Ar physisorption, TEM and temperature programmed reduction.

## 2. Experimental

### 2.1. Preparation of the catalysts

Supported Ru catalysts were obtained by incipient-wetness impregnation of zeolite H-BEA ( $\text{SiO}_2:\text{Al}_2\text{O}_3 = 25$  and 150; Clariant) as supports via  $\text{Ru}(\text{NO})(\text{NO}_3)_3$  (Alfa Aesar),  $\text{Ru}(\text{acac})_3$  (Alfa Aesar),  $\text{RuCl}_3 \cdot x\text{H}_2\text{O}$  (Alfa Aesar) and  $\text{Ru}_3(\text{CO})_{12}$  (Sigma Aldrich) as metal precursors. Using  $\text{Ru}(\text{NO})(\text{NO}_3)_3$  and  $\text{RuCl}_3 \cdot x\text{H}_2\text{O}$  water, while using  $\text{Ru}(\text{acac})_3$  and  $\text{Ru}_3(\text{CO})_{12}$  toluene was used as solvent. The samples were dried for 15 h at 373 K and reduced for 3 h in flowing hydrogen ( $50 \text{ mL g}_{\text{catalyst}}^{-1}$ ) in a temperature range of 523 K and 923 K. The nominal metal content was 1 wt.% and 2 wt.%, denoted as 1%Ru/H-BEA and 2%Ru/H-BEA, respectively. It was exemplarily validated via ICP-OES on a Varian 715-ES.

### 2.2. Ar physisorption

Surface areas were determined by Ar physisorption using the BET equation, pore volume (determined in a range until 15 nm) and micropore volume was determined by NLDFT-method (Non-Local Density Functional Theory). The samples were pre-treated under vacuum for 2 h at 353 K, for 2 h at 373 K and 20 h at 573 K. The measurements were conducted at 87 K in a range between  $p/p_0 = 10^{-6} – 0.99$  on a Quantachrome ASiQ.

### 2.3. CO chemisorption

The CO uptake and size of Ru particles were determined by CO chemisorption measurements using a TPD/R/O 1100 (Thermo Fisher Scientific). After reducing the sample at 473 K for 1 h followed by cooling down to 273 K in a hydrogen flow CO pulses ( $V = 0.473 \text{ mL}$ ) were introduced. Assuming an adsorption of one CO molecule per accessible metal atom, the amount of chemisorbed CO was determined and the metal particle size was obtained via  $d = 6 \times (\nu_m/a_m) \times D^{-1}$  with  $\nu_m$  = volume occupied by an atom in bulk metal,  $a_m$  = area occupied by a surface atom and  $D$  = dispersion [32].

### 2.4. Temperature programmed reduction

Temperature programmed reduction measurements were conducted on an apparatus TPD/R/O 1100 (Thermo Fisher Scientific). The catalysts were oxidized at 623 K for 1 h in 4.9 vol%  $\text{O}_2/\text{He}$  and pre-treated in Ar at 383 K for 1 h before the measurements. For the  $\text{H}_2$ -TPR the sample was heated from 303 K to 1173 K ( $5 \text{ K min}^{-1}$ ) in 5.1 vol%  $\text{H}_2/\text{Ar}$  while monitoring the TCD signal. TPR results are presented per gram of sample.

### 2.5. Transmissions electron microscopy

For TEM images a JEOL 2100F electron microscope operating at 200 kV was used. The samples were fixed on a copper grid-supported carbon film by depositing a dispersed ethanol solution on it.

### 2.6. Diffuse reflectance infrared Fourier transform spectroscopy

DRIFTS measurements were carried out on a Bruker Equinox55 spectrometer. To determine the nature of the acid sites, the samples were exposed to pyridine saturated in flowing nitrogen at 353 K after pre-treating in flowing  $\text{N}_2$  at 673 K (respectively 473 K for the catalysts reduced at lower temperatures).

### 2.7. X-ray Diffraction

A powder X-ray diffraction (XRD) analysis of the samples was carried out on a Mythen1K (Dectris) diffractometer using  $\text{CuK}\alpha 1$ -radiation ( $\lambda = 1.5406 \text{ \AA}$ ).

### 2.8. Catalytic experiments

The hydrogenation experiments were carried out in a stainless steel autoclave (Parr, 300 mL) usually using *n*-hexane (Roth) as solvent at 373 K and 25 bar hydrogen pressure. The reactor was charged with 0.5 g catalyst, 150 mL solvent, and 1 mL *n*-tetradecane (Merck) as internal GC standard. After reaching the desired temperature, 4.5 g racemic citronellal (Merck) was added and the reactor was pressurized via a separate tank. This was defined as the start of the reaction. Samples were taken periodically and analysed by gas chromatography (Shimadzu GC 2010 Plus) using an Agilent DB-Wax column (348 K, 5 min;  $1 \text{ K min}^{-1} \rightarrow 381 \text{ K}$ ;  $5 \text{ K min}^{-1} \rightarrow 413 \text{ K}$ ;  $20 \text{ K min}^{-1} \rightarrow 493 \text{ K}$ , 5 min). Note that it was ensured by using powdered catalysts (particle size distribution d90% of <20  $\mu\text{m}$ ) and a stirring rate of 1000 rpm that the reactions were expired under chemical control.

Conversion (X) and selectivities ( $S_i$ ) were calculated via the following equations.

$$X_{\text{CAL}} (\%) = \left( 1 - \frac{c_{\text{CAL}}}{c_{\text{CAL},0}} \right) \cdot 100 \quad (1)$$

$$S_i (\%) = \left( \frac{c_i}{c_{\text{CAL},\text{converted}}} \cdot \frac{|\nu_{\text{CAL}}|}{\nu_i} \right) \cdot 100 \quad (2)$$

The quantification of the diastereoselectivity was identified via the mole fraction ( $x_{\text{MT}}$ ) of the desired stereoisomer.

$$x_{\text{MT}} (\%) = \frac{c_{\text{Menthol}}}{\sum c_{\text{Menthols}}} \cdot 100 \quad (3)$$

Both (the turn-over-frequency (TOF) and activity of the catalyst) refer to the point of the maximum menthol selectivity. The TOF refers only to the hydrogenation step of isopulegols, the amount of active sites is obtained from CO uptake of the CO chemisorption measurements. The activity of the catalyst is calculated from the obtained amount of menthol referred to the mass of the catalyst.

$$\text{TOF} (\text{min}^{-1}) = \frac{n_{\text{Menthols,formed}}}{m_{\text{catalyst}} \cdot n_{\text{CO}} \cdot t_{\text{SMenthols,max}}} \quad (4)$$

$$\text{Activity} \left( \frac{\text{mmol}}{\text{min} \cdot \text{g}_{\text{catalyst}}} \right) = \frac{n_{\text{Menthols,formed}}}{m_{\text{catalyst}} \cdot t_{\text{SMenthols,max}}} \quad (5)$$

## 3. Results and discussion

### 3.1. Effect of the precursor

#### 3.1.1. Characterization of the catalysts

Pyridine DRIFT spectra of the 1%Ru/H-BEA-25 catalysts prepared in aqueous ( $\text{Ru}(\text{NO})(\text{NO}_3)_3$ ) and organic ( $\text{Ru}(\text{acac})_3$ ) solution are shown in Fig. 2.

Pyridine DRIFT spectra show the typical bands for H-BEA zeolites [14,33]. Bands at  $1445 \text{ cm}^{-1}$  and  $1596 \text{ cm}^{-1}$  can be assigned to

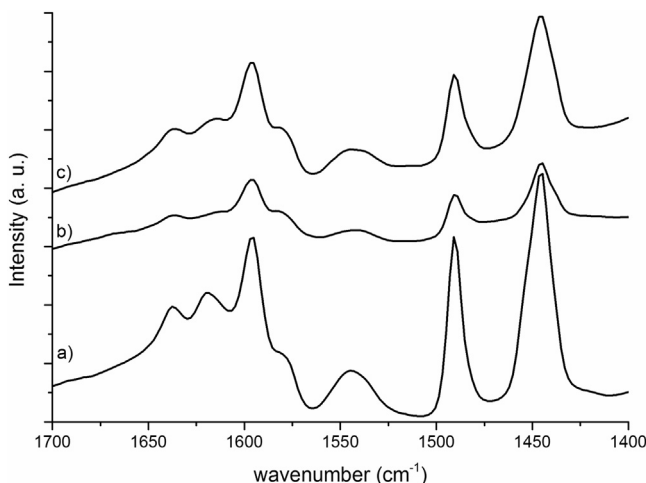


**Fig. 2.** Pyridine DRIFT spectra of (a) non-loaded H-BEA-25 and the 1%Ru/H-BEA-25 catalysts with (b) Ru(NO)(NO<sub>3</sub>)<sub>3</sub> and (c) Ru(acac)<sub>3</sub> as precursor.

hydrogen bonded pyridine, whereas the bands at 1546 cm<sup>-1</sup> and 1639 cm<sup>-1</sup> correspond to pyridinium ion ring vibration due to pyridine bound to Brønstedt acid sites. Strong Lewis bound pyridine leads to bands at 1623 cm<sup>-1</sup> and 1455 cm<sup>-1</sup>, whereas weak Lewis bonded pyridine leads to a band at 1575 cm<sup>-1</sup>. Additionally to this band at 1492 cm<sup>-1</sup> can be assigned to pyridine associated with both Brønstedt and Lewis acid sites [33,34].

Unloaded H-BEA shows strong Lewis bound pyridine (1623 cm<sup>-1</sup>), which disappears after loading with Ru and reduction, but no significant difference between the catalysts prepared from Ru(NO)(NO<sub>3</sub>)<sub>3</sub> and Ru(acac)<sub>3</sub> were detected via pyridine DRIFTS.

**Table 1** summarizes the main properties of different catalysts as Ru loading obtained via ICP measurements, the CO uptake and size of the Ru particles obtained via CO chemisorption as well as the surface area and pore volumina obtained from Ar physisorption.

The loadings of the catalysts, estimated by ICP-OES, differ slightly from the nominal Ru content which may be ascribed to the formation of volatile intermediates during thermal pretreatment and/or the type of chemical digestion.

The size of the Ru particles is amounted to 1.3–2 nm, with the expectation of the catalyst prepared from RuCl<sub>3</sub> as its particles are significantly larger with 5.4 nm. This can be attributed to Cl<sup>-</sup> ions, which are known to cause larger particles [26].

The values for the catalyst prepared from Ru(NO)(NO<sub>3</sub>)<sub>3</sub> and Ru(acac)<sub>3</sub> obtained from CO chemisorption are confirmed by TEM images (Fig. 6). The impregnation with Ru does not strongly effect the surface area and pore volume, which indicates no blockage of the zeolite pores.

In conclusion, the Ru particle size is affected by the precursor. RuCl<sub>3</sub> leads to the largest particles of 5.4 nm, whereas Ru(NO)(NO<sub>3</sub>)<sub>3</sub> leads to the smallest particles of 1.3 nm. The surface area of the catalyst is slightly increased when loaded with Ru, but no significant difference between the catalysts prepared from Ru(NO)(NO<sub>3</sub>)<sub>3</sub> and Ru(acac)<sub>3</sub> were detected via pyridine DRIFTS.

### 3.1.2. Effect on the formation of menthols

For the one-pot transformation of menthols from citronellal on 1%Ru/H-BEA catalysts the effect of the Ru precursor was investigated. RuNO(NO<sub>3</sub>)<sub>3</sub>, Ru(acac)<sub>3</sub>, RuCl<sub>3</sub> and Ru<sub>3</sub>(CO)<sub>12</sub> were used as precursors. **Table 2** summarizes the time for reaching the maximum selectivity to menthols, selectivities to menthols ( $S_{MTs}$ ), isopulegols ( $S_{ISPs}$ ), hydrogenation products of citronellal ( $S_{Hyd.}$ ), defunctionalization ( $S_{DFP}$ ) and dimerization products ( $S_{Dimers}$ ) as well as diastereoselectivity to menthol ( $x_{MT}$ ) and activities of menthol for-

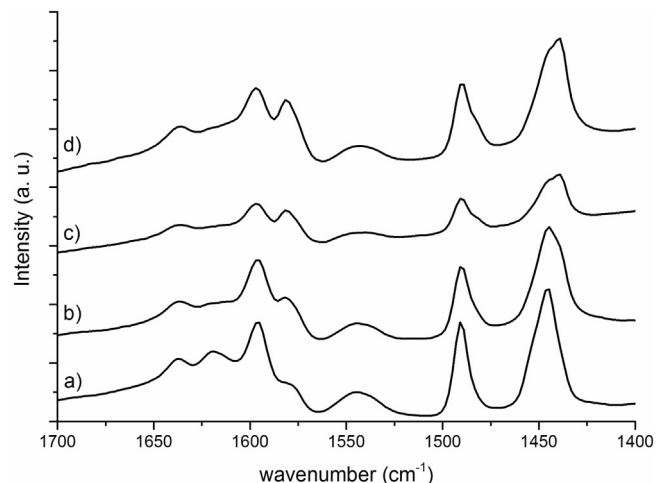


**Fig. 3.** Pyridine DRIFT spectra of (a) H-BEA-25 (b) 2%Ru/H-BEA-25 reduced at 623 K (c) H-BEA-25 reduced at 923 K and (d) 2%Ru/H-BEA-25 reduced at 923 K.

mation in the one-pot synthesis of menthol on 1%Ru/H-BEA-25 catalysts prepared from different Ru precursors.

Note, because of the fast cyclization of citronellal (see Fig. 8) a full conversion is reached after a few minutes. Because of the consecutive reaction (Fig. 1, route 1 and 2), the maximum selectivity to menthols is reached at the point when the intermediate isopulegol is totally converted. This point is reached after 120 min for the catalyst prepared from Ru(NO)(NO<sub>3</sub>)<sub>3</sub>, while the catalyst prepared from Ru(acac)<sub>3</sub> needs 300 min to reach this point. This leads to activities of 0.37 mmol g<sub>cat</sub><sup>-1</sup> min<sup>-1</sup> – 0.16 mmol g<sub>cat</sub><sup>-1</sup> min<sup>-1</sup> and TOFs of 1.7 min<sup>-1</sup> for the catalyst prepared from Ru(acac)<sub>3</sub> to 13.8 min<sup>-1</sup> for the catalyst prepared from RuCl<sub>3</sub>. The highest selectivity to the group of menthols of 83% can be obtained using RuCl<sub>3</sub> and Ru<sub>3</sub>(CO)<sub>12</sub> as precursor. Using Ru(NO)(NO<sub>3</sub>)<sub>3</sub> and Ru(acac)<sub>3</sub> lower selectivities of 77% respectively 82% are reached. Using Ru(NO)(NO<sub>3</sub>)<sub>3</sub> as precursor the main by-products are hydrogenation products of citronellal (mainly DMO).

The high amount of hydrogenation products formed on this catalyst can be traced back to the obviously higher Ru content of the catalyst (Table 1). A diastereoselectivity to the desired menthol stereoisomer ( $x_{MT}$ ) of about 68–73% for all catalysts. As seen in Table 1 Ru particles prepared from RuCl<sub>3</sub> are significantly larger than particles prepared from other precursors. Therefore no dependency of the product distribution and the particle size can be observed.

In summary it can be concluded that the precursor does not strongly affect the maximum selectivity to menthol, differences between the selectivities can be traced back to differences in Ru contents of the catalysts. However the precursor effects strongly the activity of the catalyst. Reaching the highest activity with Ru(NO)(NO<sub>3</sub>)<sub>3</sub> and comparing the catalysts with previous work [6] this precursor was used for further investigation.

### 3.2. Effect of the reduction temperature

#### 3.2.1. Characterization of the catalysts

Pyridine DRIFTS measurements of H-BEA-25 and 2%Ru/H-BEA-25 catalysts reduced at different temperatures are shown in Fig. 3.

Unloaded H-BEA shows strong Lewis bound pyridine (1623 cm<sup>-1</sup>), which disappears after loading with Ru and reduction at 623 K.

A band at 1575 cm<sup>-1</sup>, which can be assigned to weak Lewis bound pyridine [34], rises with increasing reduction temperature for both the loaded and non-loaded zeolite. The latter may be either traced back to the elimination of H<sub>2</sub>O from the zeolite framework

**Table 1**

Effect of the precursor on Ru loading, CO uptake, Ru particle size, pore volumina and surface area of 1%Ru/H-BEA-25 reduced at 623 K.

#	Precursor	Ru loading <sup>a</sup> (wt%)	CO uptake <sup>b</sup> (μmol g <sup>-1</sup> ) and size of Ru particles <sup>b</sup> in parentheses (nm)	Surface area <sup>c</sup> (m <sup>2</sup> g <sup>-1</sup> )	Pore volume <sup>c</sup> /cm <sup>3</sup> g <sup>-1</sup>	Micropore volume <sup>c</sup> /cm <sup>3</sup> g <sup>-1</sup>
1	— <sup>d</sup>	0	0	482	0.409	0.217
2	Ru(NO)(NO <sub>3</sub> ) <sub>3</sub>	1.35	134 (1.3)	478	0.400	0.209
3	Ru(acac) <sub>3</sub>	1.09	97 (1.4)	483	0.395	0.217
4	RuCl <sub>3</sub>	0.83	19 (5.4)	n.d.	n.d.	n.d.
5	Ru <sub>3</sub> (CO) <sub>12</sub>	0.91	58 (2.0)	n.d.	n.d.	n.d.

<sup>a</sup> Obtained from ICP measurements.

<sup>b</sup> Obtained from CO Chemisorption.

<sup>c</sup> Obtained from Ar Physisorption.

<sup>d</sup> Non-loaded H-BEA-25.

**Table 2**

Effect of the precursor on product selectivities and activities of menthol formation in the one-pot synthesis of menthols on 1%Ru/H-BEA-25 reduced at 623 K.<sup>a</sup>

#	Precursor	t <sub>max</sub> <sup>b</sup> (min)	S <sub>MTs</sub> (%)	S <sub>ISPs</sub> (%)	S <sub>Hyd.</sub> <sup>c</sup> (%)	S <sub>DFF</sub> <sup>d</sup> (%)	S <sub>Dimers</sub> (%)	x <sub>MTs</sub> (%)	Activity <sup>e</sup> (mmol min <sup>-1</sup> g <sub>cat</sub> <sup>-1</sup> )	TOF <sup>f</sup> (min <sup>-1</sup> )
1	Ru(NO)(NO <sub>3</sub> ) <sub>3</sub>	120	77	0	18	1	5	69	0.37	2.8
2	Ru(acac) <sub>3</sub>	300	82	1	8	3	6	68	0.16	1.7
3	RuCl <sub>3</sub>	180	83	2	5	3	7	73	0.27	13.8
4	Ru <sub>3</sub> (CO) <sub>12</sub>	180	83	1	6	3	7	73	0.27	4.7

<sup>a</sup> Reaction conditions: 4.5 g CAL, 0.5 g 1%Ru/H-BEA-25, 150 mL n-hexane, 1 mL n-tetradecane, 25 bar, 373 K.

<sup>b</sup> X<sub>CAL</sub> = 100%.

<sup>c</sup> S<sub>Hyd.</sub> = S<sub>DHC</sub> + S<sub>COL</sub> + S<sub>DMO</sub>.

<sup>d</sup> S<sub>DFF</sub> = sum of defunctionalized products (mainly p-menthenes and p-menthanes).

<sup>e</sup> The activity is calculated from the obtained amount of menthol referred to the mass of the catalyst and the time referred to the maximum selectivity to menthols.

<sup>f</sup> The TOF refers to the hydrogenation of isopulegols to menthols at the point of the maximum selectivity to menthols. The amount of active sites is obtained from CO uptake of the CO chemisorption measurements.

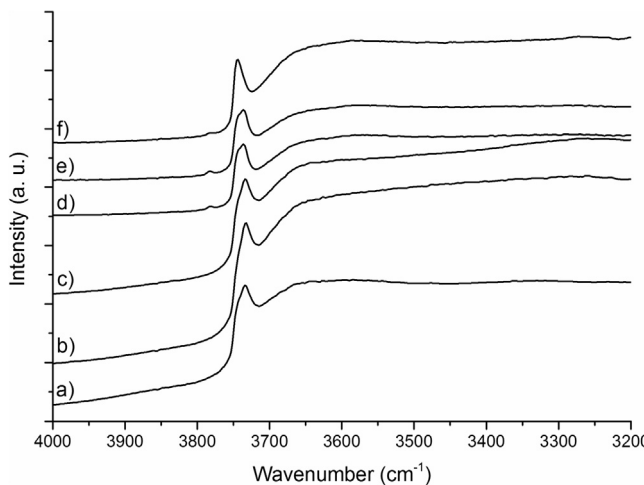


**Fig. 4.** DRIFT spectra of the O—H-stretching region of (a) H-BEA-25 and 1%Ru/H-BEA-25 reduced at (b) 523 K (c) 623 K (d) 723 K (e) 823 K and (f) 923 K.

forming new Lewis acid sites during the high temperature reduction process [33] and/or a (partial) dealumination of the zeolite [28]. It was also reported by Lenarda et al. [28] the total number of acid sites of zeolite BEA (determined via TPD of ammonia and FT-IR of adsorbed pyridine) decreases with increasing treatment temperature, while the amount of Brønsted acid sites decreases more rapidly. Consequently the ratio of Lewis to Brønsted acid sites slightly increases.

Supporting Ru on zeolite H-BEA-25 (in addition the amount of supported Ru, Fig. 2b) does not affect the spectra significantly. However, reduction temperature strongly influences the nature of the acid sites very much.

DRIFT spectra of the O—H-stretching region of H-BEA and 1%Ru/H-BEA reduced at different temperatures are shown in Fig. 4.

Three bands corresponding to different OH-groups are observed. A main sharp band corresponding to silanols with two resolved

components is observed at 3735 cm<sup>-1</sup> (OH groups in lattice defects/internal surface [29,30]) and 3744 cm<sup>-1</sup> (terminal OH groups on the external surface [30]). A sharp band at 3785 cm<sup>-1</sup> may be associated with Al-OH groups corresponding to EF-Al groups [29,35,36] or to OH on partially hydrolysed aluminium sites, which are bounded to the framework via one or two oxygen bonds [30,35,36]. In agreement with Trombetta et al. [29] the treatment at higher temperatures leads to a decrease in the bands at 3735 cm<sup>-1</sup> and to an increase of the bands at 3744 cm<sup>-1</sup> and 3785 cm<sup>-1</sup> indicating a dealumination of the zeolite. In the same work it was demonstrated via <sup>27</sup>Al-MAS-NMR that zeolite BEA treated at high temperatures showed- additionally to tetrahedrally coordinated aluminium- signals corresponding to octahedral and pentacoordinated aluminium respectively to Al atoms in highly distorted tetrahedral coordination. After treating the sample with acids, only tetrahedrally coordinated aluminium retained, which confirms the assumption of a progressive dealumination of the zeolite framework at high temperatures [29].

XRD patterns of zeolite H-BEA-25 and 2%Ru/H-BEA-25 reduced at 623 K and 923 K are shown in Fig. 5.

No reflexes corresponding to Ru are detected, which indicates a high dispersion of Ru particles on the zeolite. However, the zeolite is not highly crystalline [37], the crystallinity of the zeolite retained during the reduction at high temperatures. A shift of the signal positions described by Trombetta et al. [29] cannot be detected due to the low crystallinity.

**Table 3** summarizes the main properties of the different catalysts such as Ru loading obtained via ICP measurements, the CO uptake and the size of the Ru particles obtained via CO chemisorption as well as surface area and pore volumina obtained from Ar physisorption.

The constant Ru amount obtained via ICP measurements demonstrates the stability of Ru up to high reduction temperatures, no volatile components are formed during the reduction process. For H-BEA-25, the CO uptake decreases slightly with rising reduction temperature, whereas it increases for H-BEA-150. However it

**Table 3**

Effect of the reduction temperature on Ru loading, CO uptake, Ru particle size, pore volumina and surface area on Ru/H-BEA catalysts.

#	Catalyst	Ru loading <sup>a</sup> (wt%)	CO uptake <sup>b</sup> ( $\mu\text{mol g}^{-1}$ ) and size of Ru particles <sup>b</sup> in parentheses (nm)	Surface area <sup>c</sup> ( $\text{m}^2 \text{g}^{-1}$ )	Pore volume <sup>c</sup> / $\text{cm}^3 \text{g}^{-1}$	Micropore volume <sup>c</sup> / $\text{cm}^3 \text{g}^{-1}$
1	H-BEA-25 <sup>d</sup>	0	0 (–)	482	0.409	0.217
2	1%Ru/H-BEA-25 (623 K)	1.35	134 (1.3)	478	0.400	0.209
3	1%Ru/H-BEA-25 (773 K)	n.d.	119 (1.4)	n.d.	n.d.	n.d.
4	1%Ru/H-BEA-25 (923 K)	1.36	121 (1.4)	498	0.400	0.213
5	2%Ru/H-BEA-25 (623 K)	n.d.	167 (1.5)	492	0.386	0.216
6	2%Ru/H-BEA-25 (923 K)	n.d.	164 (1.5)	523	0.407	0.227
7	H-BEA-150 <sup>d</sup>	0	0 (–)	548	0.380	0.243
8	2%Ru/H-BEA-150 (623 K)	2.28	119 (2.5)	558	0.395	0.256
9	2%Ru/H-BEA-150 (923 K)	n.d.	187 (1.6)	n.d.	n.d.	n.d.

<sup>a</sup> Obtained from ICP measurements.

<sup>b</sup> Obtained from CO Chemisorption.

<sup>c</sup> Obtained from Ar Physisorption.

<sup>d</sup> Non-loaded H-BEA.

**Table 4**

Effect of the reduction temperature of Ru/H-BEA (precursor: RuNO(NO<sub>3</sub>)<sub>3</sub>) on product selectivities and activities of menthol formation in the one-pot synthesis of menthol.<sup>a</sup>

#	Loading (wt%)	SiO <sub>2</sub> :Al <sub>2</sub> O <sub>3</sub>	T <sub>Red</sub> (K)	t <sub>Smax</sub> <sup>b</sup> (min)	S <sub>MTs</sub> (%)	S <sub>ISPs</sub> (%)	S <sub>Hyd.</sub> <sup>c</sup> (%)	S <sub>DFFP</sub> <sup>d</sup> (%)	S <sub>Dimers</sub> (%)	Activity <sup>e</sup> (mmol min <sup>-1</sup> g <sub>cat</sub> <sup>-1</sup> )	TOF <sup>f</sup> (min <sup>-1</sup> )
1	1	25	523	300	72	2	21	1	4	0.14	1.0
2	1	25	623	120	77	0	18	1	5	0.37	2.8
3	1	25	723	60	82	2	11	2	3	0.80	5.4
4	1	25	773	60	87	1	8	3	2	0.84	7.1
5	1	25	823	60	85	0	9	3	2	0.83	5.8
6	1	25	923	40	87	1	9	2	2	1.27	10.5
7	2	25	523	300	43	6	49	0	2	0.08	0.4
8	2	25	623	120	54	0	41	1	3	0.26	1.6
9	2	25	723	60	69	0	26	2	3	0.67	3.7
10	2	25	823	60	64	1	26	3	6	0.62	3.7
11	2	25	923	40	79	1	16	3	1	1.15	7.0
12	2	150	623	40	65	1	26	2	5	0.95	8.0
13	2	150	923	20	85	1	12	1	1	2.48	13.3

<sup>a</sup> Reaction conditions: 4.5 g CAL, 0.5 g Ru/H-BEA, 373 K, 150 mL n-hexane, 1 mL n-tetradecane, 25 bar, 373 K.

<sup>b</sup> X<sub>CAL</sub> = 100%.

<sup>c</sup> S<sub>Hyd.</sub> = S<sub>DHC</sub> + S<sub>COL</sub> + S<sub>DMO</sub>.

<sup>d</sup> S<sub>DFFP</sub> = sum of defunctionalized products (mainly p-menthenes and p-menthanes).

<sup>e</sup> The activity is calculated from the obtained amount of menthol referred to the mass of the catalyst and the time referred to the maximum selectivity to menthols.

<sup>f</sup> The TOF refers to the hydrogenation of isopulegols to menthols at the point of the maximum selectivity to menthols. The amount of active sites is obtained from CO uptake of the CO chemisorption measurements.

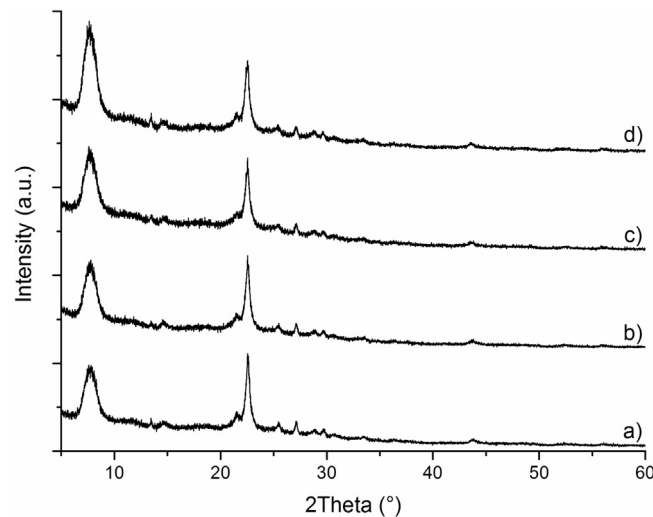


**Fig. 5.** XRD pattern of (a) H-BEA-25 (b) 2%Ru/H-BEA-25 reduced at 623 K (c) H-BEA-25 reduced at 923 K and (d) 2%Ru/H-BEA-25 reduced at 923 K.

is only less affected by the reduction temperature, the size of the Ru particles on 1%Ru/H-BEA-25 grows slightly from 1.3 nm to 1.4 nm. After loading the zeolite with Ru and reducing it at various temperatures, both the pore volume and micropore volume remains

constant, whereas the surface area increases with the reduction temperature. After reduction of 1%Ru/H-BEA-25 at 623 K a surface area of 478  $\text{m}^2 \text{g}^{-1}$  is detected, reduction at 923 K leads to a surface area of 498  $\text{m}^2 \text{g}^{-1}$ , whereas the surface area of the 2%Ru/H-BEA-25 catalyst increases up to 523  $\text{m}^2 \text{g}^{-1}$  after reduction at 923 K. The increase in the surface area with rising reduction temperature is consistent with previous works on dealuminated zeolite BEA [29].

TEM images (Fig. 6) confirm the particle size of about 1–2 nm obtained from CO chemisorption.

Temperature programmed reduction was carried out on 1%Ru/H-BEA-25 reduced at 623 K, 773 K and 923 K (Fig. 7). With increasing reduction temperature, the reduction peak shifts to lower temperatures (437 K → 423 K), which additionally indicates a dealumination of the zeolite framework. Lashdaf et al. [38] reported a dependency of the maximum in the hydrogen consumption in TPR analysis from the Si:Al ratio of zeolite BEA. In addition Vasiliadou et al. [27] reported a reduction peak at lower temperatures for Ru supported on SiO<sub>2</sub> than on Al<sub>2</sub>O<sub>3</sub>.

Pyridine DRIFTS measurements show an increase of the amount of Lewis acid sites when reduction temperature for both the loaded and non-loaded zeolite was risen. DRIFTS measurements, the increasing surface area and TPR analysis indicate dealumination of the zeolite framework. Ru content and particle size are marginally affected by reduction temperature. CO chemisorption measurements and TEM images confirm that no sintering of the Ru particles occurs.

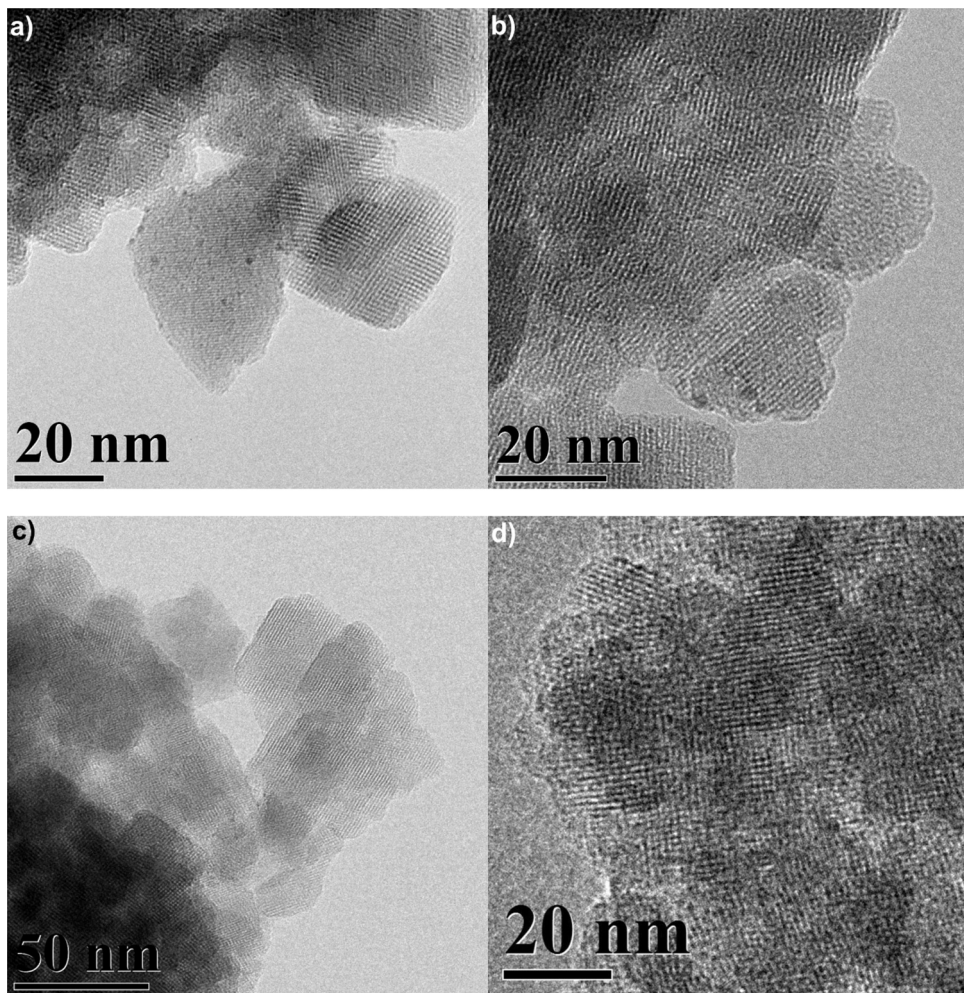


**Fig. 6.** TEM images of 1%Ru/H-BEA (a) precursor: Ru(acac)<sub>3</sub> reduced at 623 K (b) and (c) precursor: Ru(NO)(NO<sub>3</sub>)<sub>3</sub> reduced at 623 K and d) precursor: Ru(NO)(NO<sub>3</sub>)<sub>3</sub> reduced at 923 K.

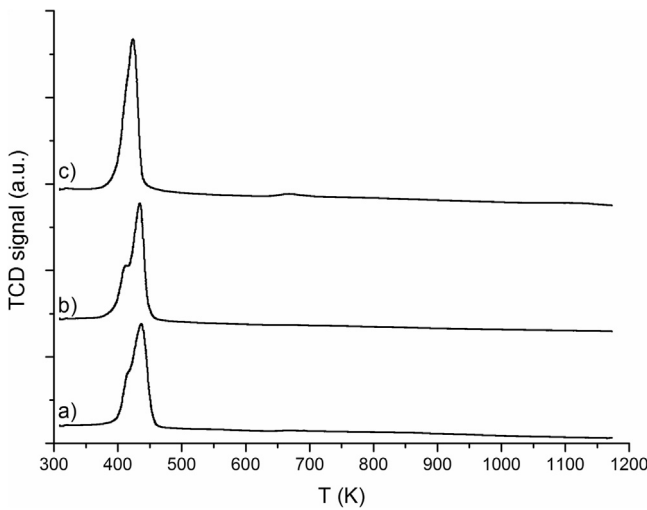


**Fig. 7.** TPR profile of 1%Ru/H-BEA-25 catalysts reduced at (a) 623 K (b) 773 K and (c) 923 K.

### 3.2.2. Effect to the formation of menthol

In the next step the effect of reduction temperature to formation of menthols from citronellal of Ru/H-BEA was investigated. It was varied in a range of 523 K and 923 K, Ru loadings of 1 wt% and 2 wt% as well as SiO<sub>2</sub>:Al<sub>2</sub>O<sub>3</sub> ratios of 25 and 150 were used.

**Table 4** summarizes the time for reaching the maximum selectivities to menthols, selectivities to menthols ( $S_{MTS}$ ), isopulegols ( $S_{ISP_S}$ ), hydrogenation products of citronellal ( $S_{Hyd\_}$ ), defunctionalization ( $S_{DFP}$ ) and dimerization products ( $S_{Dimers}$ ) as well as activities of menthol formation in the one-pot synthesis of menthol on Ru/H-BEA catalysts reduced at various temperatures. For each catalyst the obtained diastereoselectivity is about 70% and therefore it is not listed here in detail.

Note, because of the fast cyclization of citronellal a full conversion is reached after a few minutes. The higher the reduction temperature of the catalyst is the higher the activity for each catalyst. Increasing the reduction temperature of a 1%Ru/H-BEA-25 catalyst from 623 K to 923 K the activity increases by a factor of 3.4, the TOF increases with a factor of 3.8. This leads to a reaction time of 40 min instead of 120 min for the maximum selectivity.

But more important than the activity is the higher selectivity to menthols. Whereas a menthol selectivity of only 77% is reached with the 1%Ru/H-BEA-25 catalyst reduced at 623 K, a selectivity of 87% is reached with the same catalyst reduced at 923 K. The same trends are observed for 2%Ru/H-BEA catalysts with a SiO<sub>2</sub>:Al<sub>2</sub>O<sub>3</sub> ratio of 25 and 150. For example the maximum menthol selectivity increases from 54% for the catalyst reduced at 623 K to 79% for the catalyst reduced at 923 K. The increased menthol selectivity is accompanied by a reduced formation of unwanted hydrogenation products. For the 1%Ru/H-BEA-25 catalyst the selectivity to hydrogenation products decreases from 18% (reduced at 623 K) to

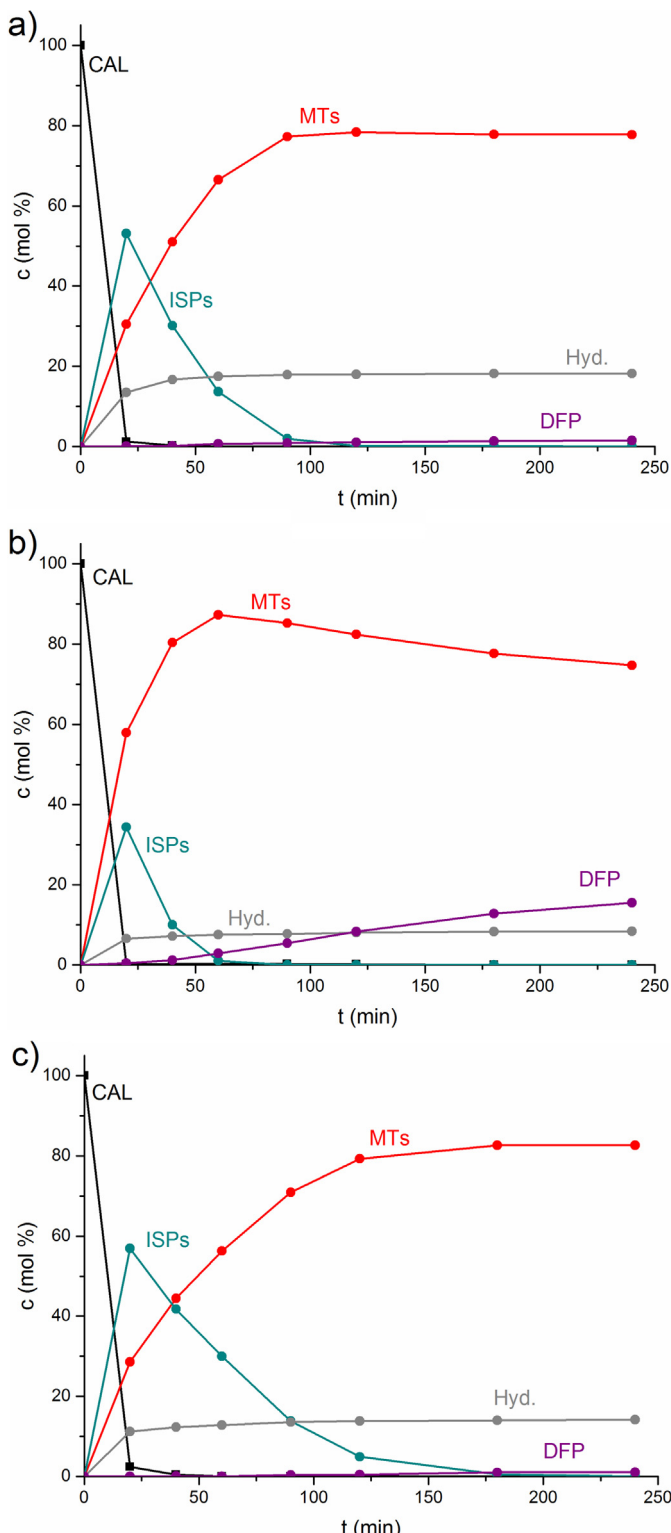


**Fig. 8.** Concentration of citronellal, isopulegols, hydrogenation products and defunctionalization products during the one-pot transformation of citronellal to menthol on 1%Ru/H-BEA-25. (a) Reduced at 623 K (b) reduced at 773 K (c) zeolite pre-reduced at 773 K-catalyst reduced at 623 K. (Reaction conditions: 4.5 g CAL, 0.5 g catalyst, 150 mL *n*-hexane, 1 mL *n*-tetradecane, 25 bar, 373 K).

9% (reduced at 923 K), for the 2%Ru/H-BEA-25 catalyst it decreases from 41% (reduced at 623 K) to 16% (reduced at 923 K).

Fig. 8 demonstrates the accelerated formation of menthols on 1%Ru/H-BEA-25 catalysts reduced at higher temperatures. On the

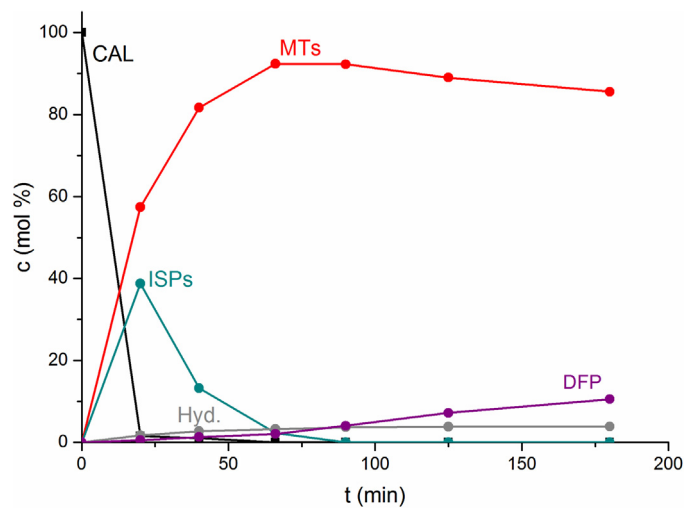


**Fig. 9.** Concentration of citronellal, isopulegols, hydrogenation products and defunctionalization products during the one-pot transformation of citronellal to menthol on 1%Ru/H-BEA reduced at 923 K using optimized conditions (Reaction conditions: 4.5 g CAL, 0.5 g catalyst, 150 mL *n*-dioxane, 1 mL *n*-tetradecane, 25 bar, 373 K).

catalyst reduced at 623 K the maximum selectivity to menthols of 77% is obtained after 120 min (Fig. 8a), whereas using 1%Ru/H-BEA-25 catalysts reduced at 773 K the maximum selectivity of 87% is obtained after only 60 min (Fig. 8b).

As seen in Fig. 1 the distribution of the selectivities concerning hydrogenation products and isopulegols/menthols is determined in the first step: The cyclization of citronellal (route 1) competes with its hydrogenation (route 3). For the catalyst reduced at higher temperatures the cyclization is favoured and therefore less hydrogenation products are formed. As indicated above the zeolite is dealuminated during the reduction at higher temperatures forming weak Lewis acid sites. Comparing 2%Ru/H-BEA catalysts with different Si:Al ratios (Table 4, line 8 vs. 12 and reported in our previous study [6]) demonstrates that increasing the Si:Al ratio of the zeolite enhances the menthol selectivity and activity of the catalyst. To evaluate, if the enhanced catalyst performance of the catalyst reduced at higher temperatures is a result of an increased Si:Al ratio of the zeolite network, zeolite H-BEA was pre-reduced at 773 K before impregnation with Ru( $\text{NO}_3$ )<sub>3</sub> and the following reduction at 623 K. This catalyst leads to a selectivity vs. time plot similar to the catalyst reduced at 623 K (Fig. 8c vs. Fig. 8a). However an increase of the maximum menthol selectivity from 77% to 81% is observed, but activity of the catalyst remains constant. Therefore it is demonstrated, that the enhanced performance is not just a result of the increased Si:Al ratio. Consequently it is necessary to reduce both- the zeolite and Ru- together at high temperatures to enhance the activity and selectivity of the catalyst in the one-pot transformation of citronellal to menthols.

As demonstrated above reducing pure zeolite H-BEA at high temperatures leads also to a dealumination. It can be assumed that dealuminated species promote cyclization of citronellal and are located closely to the Ru particles. Consequently cyclization of citronellal is favoured to its hydrogenation and the formed isopulegols can be hydrogenated immediately and therefore the reaction occurs faster. However, interaction between Ru and dealuminated species has to be investigated in a further study, it can be assumed that the contact between both is necessary for an enhanced catalytic performance.

Additionally, reducing the catalyst at higher temperature leads to high amounts of defunctionalized products. In our previous study [6] we demonstrated that defunctionalization predomi-

nates on Ru/H-BEA catalysts with high Si:Al ratios, which are less Brønstedt acidic. Therefore it can be assumed that Lewis acids favour defunctionalization. Pre-reducing the zeolite additionally decelerates hydrogenation of isopulegols slightly.

It is known from prior studies that the formation of menthols is favoured when using dioxane as solvent [6,24]. Therefore a 1%Ru/H-BEA-25 catalyst reduced at 923 K was used with dioxane as solvent. Due to the lower solubility of hydrogen in dioxane [39] isopulegols are hydrogenated slower than in *n*-hexane, which leads to and also a lower activity ( $0.90 \text{ mmol min}^{-1} \text{ g}_{\text{cat}}^{-1}$  vs.  $1.27 \text{ mmol min}^{-1} \text{ g}_{\text{cat}}^{-1}$ ). But an excellent yield of 92% and diastereoselectivity to the desired menthol stereoisomer of 79% was reached after 60 min (Fig. 9).

Little amounts of undesired hydrogenation and defunctionalization products are detected.

This results show the importance of an appropriate preparation procedure of the catalyst as well as the interaction with appropriate reaction conditions.

#### 4. Conclusion

The one-pot transformation of citronellal to menthols was successfully achieved on heterogeneous Ru/H-BEA catalysts. In a first step, on a 1%Ru/H-BEA catalyst the effect of different Ru precursors ( $\text{Ru}(\text{NO})(\text{NO}_3)_3$ ,  $\text{Ru}(\text{acac})_3$ ,  $\text{RuCl}_3$  and  $\text{Ru}_3(\text{CO})_{12}$ ) was investigated.

The highest activity was obtained by using  $\text{Ru}(\text{NO})(\text{NO}_3)_3$ . The highest selectivities were reached with  $\text{RuCl}_3$  and  $\text{Ru}_3(\text{CO})_{12}$ , whereas hydrogenation products of citronellal were the predominant group of by-products for all catalysts. The latter was assigned with higher Ru content of the catalyst prepared from  $\text{Ru}(\text{NO})(\text{NO}_3)_3$ .

Significant effects were observed by varying the reduction temperature. By increasing it from 623 K to 923 K for a 1%Ru/H-BEA-25 catalyst (using  $\text{Ru}(\text{NO})(\text{NO}_3)_3$  as precursor) the selectivity to menthols rises from 77% to 87%. Similar activity of the catalyst increases with a factor of 3.4. Pyridine DRIFTS, DRIFTS and Ar physisorption measurements indicate a dealumination of the zeolite at higher reduction temperatures. Pre-treating the zeolite at high temperatures before impregnating it with the Ru precursor does not effect a higher performance. Thus it was demonstrated that zeolite and Ru have to be reduced together and the enhanced performance is not just a result of an increased Si:Al ratio. When combining the new developed catalyst system with appropriate reaction conditions (dioxane as solvent) the menthols were obtained in excellent yield of 92%.

#### Acknowledgements

We thank Kathrin Hofmann for XRD measurements, Alexander Zintler for TEM analyses, Quantachrome for Ar physisorption and LIKAT for ICP measurements.

#### References

- [1] J.C. Leffingwell, Handb. Cosmet. Sci. Technol. 3 (2009) 661–675.
- [2] B. Schäfer, Chem. unserer Zeit. 47 (2013) 174–182.
- [3] R.G. Jacob, G. Perin, L.N. Loi, C.S. Pinno, E.J. Lenardão, Tetrahedron Lett. 44 (2003) 3605–3608.
- [4] C. Milone, A. Perri, A. Pistone, G. Neri, S. Galvagno, Appl. Catal. A 233 (2002) 151–157.
- [5] M. Vandichel, F. Vermoortele, S. Cottenie, D.E. De Vos, M. Waroquier, V. Van Speybroeck, J. Catal. 305 (2013) 118–129.
- [6] J. Plößer, M. Lucas, P. Claus, J. Catal. 320 (2014) 189–197.
- [7] F. Neațu, S. Coman, V.I. Pârvulescu, G. Poncelet, D. De Vos, P. Jacobs, Top Catal. 52 (2009) 1292–1300.
- [8] P.R. Braga, A.A. Costa, E.F. de Freitas, R.O. Rocha, J.L. de Macedo, A.S. Araujo, J.A. Dias, S.C. Dias, J. Mol. Catal. A: Chem. 358 (2012) 99–105.
- [9] K.A. da Silva, P.A. Robles-Dutenhefner, E.M.B. Sousa, E.F. Kozhevnikova, I.V. Kozhevnikov, E.V. Gusevskaya, Catal. Commun. 5 (2004) 425–429.
- [10] G.K. Chuah, S.H. Liu, S. Jaenicke, L.J. Harrison, J. Catal. 200 (2001) 352–359.
- [11] C.B. Cortés, V.T. Galván, S.S. Pedro, T.V. García, Catal. Today 172 (2011) 21–26.
- [12] I. Fatimah, J. App. Sci. Res. 5 (2009) 1277–1284.
- [13] M. Fuentes, J. Magraner, C. De Las Pozas, R. Roque-Malherbe, J.P. Pariente, A. Corma, Appl. Catal. 47 (1989) 367–374.
- [14] P. Mäki-Arvela, N. Kumar, V. Nieminen, R. Sjöholm, T. Salmi, D.Y. Murzin, J. Catal. 225 (2004) 155–169.
- [15] Z. Yongzhong, N. Yuntong, S. Jaenicke, G.-K. Chuah, J. Catal. 229 (2005) 404–413.
- [16] A. Corma, M. Renz, Chem. Commun. (2004) 550–551.
- [17] D.-L. Shieh, C.-C. Tsai, A.-N. Ko, React. Kinet. Catal. Lett. 79 (2003) 381–389.
- [18] E.D. Ifitihah, W.T. Muchalal, R. Armundanto, J. Basic Appl. Sci. Res. 1 (2010) 777–781.
- [19] C. Milone, C. Gangemi, G. Neri, A. Pistone, S. Galvagno, Appl. Catal. A 199 (2000) 239–244.
- [20] A.M. Balu, J.M. Campelo, R. Luque, A.A. Romero, Org. Biomol. Chem. 8 (2010) 2845–2849.
- [21] K.A. da Silva Rocha, P.A. Robles-Dutenhefner, E.M.B. Sousa, E.F. Kozhevnikova, I.V. Kozhevnikov, E.V. Gusevskaya, Appl. Catal. A 317 (2007) 171–174.
- [22] A. Negoi, S. Wuttke, E. Kemnitz, D. Macovei, V.I. Pârvulescu, C.M. Teodorescu, S.M. Coman, Angew. Chem. Int. Ed. 49 (2010) 8134–8138.
- [23] Y. Nie, W. Niah, S. Jaenicke, G.-K. Chuah, J. Catal. 248 (2007) 1–10.
- [24] P. Mertens, F. Verpoort, A.-N. Pârvulescu, D. De Vos, J. Catal. 243 (2006) 7–13.
- [25] F. Iosif, S. Coman, V. Pârvulescu, P. Grange, S. Delsarte, D. De Vos, P. Jacobs, Chem. Commun. (2004) 1292–1293.
- [26] B. Bachiller-Baeza, A. Guerrero-Ruiz, I. Rodríguez-Ramos, J. Catal. 229 (2005) 439–445.
- [27] E.S. Vasiliadou, E. Heracleous, I.A. Vasalos, A.A. Lemonidou, Appl. Catal. B 92 (2009) 90–99.
- [28] M. Lenarda, M. Da Ros, M. Casagrande, L. Storaro, R. Ganzerla, Inorg. Chim. Acta 349 (2003) 195–202.
- [29] M. Trombetta, G. Busca, L. Storaro, M. Lenarda, M. Casagrande, A. Zambon, PCCP 2 (2000) 3529–3537.
- [30] I. Kiricsi, C. Flego, G. Pazzuconi, W.J. Parker, R. Millini, C. Perego, G. Bellussi, J. Phys. Chem. 98 (1994) 4627–4634.
- [31] M. Casagrande, L. Storaro, M. Lenarda, R. Ganzerla, Appl. Catal. A 201 (2000) 263–270.
- [32] G. Bergeret, P. Gallezot, Handbook of Heterogeneous Catalysis, Wiley-VCH Verlag GmbH & Co. KGaA, 2008 (p. 738).
- [33] T. Barzetti, E. Sellì, D. Moscotti, L. Forni, J. Chem. Soc. Faraday Trans. 92 (1996) 1401–1407.
- [34] B. Chakraborty, B. Viswanathan, Catal. Today 49 (1999) 253–260.
- [35] C. Yang, Q. Xuaf, Zeolites 19 (1997) 404–410.
- [36] A. Vimont, F. Thibault-Starzyk, J. Lavalle, J. Phys. Chem. B 104 (2000) 286–291.
- [37] J. Weitkamp, R. Kumar, S. Ernst, Chem. Ing. Tech. 61 (1989) 731–733.
- [38] M. Lashdaf, M. Tiitta, T. Venäläinen, H. Österholm, A.O.I. Krause, Catal. Lett. 94 (2004) 7–14.
- [39] E. Brunner, J. Chem. Eng. Data 30 (1985) 269–273.